SPE 81465

Effect of Gravity on Waterflooding Performance of Stratified Reservoirs

Noaman A.F. El-Khatib, SPE, King Saud University

This paper was prepared for presentation at the SPE 13th Middle east Oil Show & Conference to be held in Bahrain 5-8 April 2003.

Abstract

In this paper, an analytical solution is developed for waterflooding performance of stratified reservoirs with gravitational (bouncy) effects between adjacent layers. The ordering of layers is kept unchanged as obtained from core analysis or well logging or as randomly sampled from a specified distribution (usually a log-normal). Differential equations are obtained and solved for the rate of advance of the displacement fronts in two or three successive layers of decreasing permeability. The locations of the displacement fronts are used to obtain expressions for the time of water breakthrough in the successive layers and oil recovery factor and water cut at the time of breakthrough in the different layers.

The effect of mobility ratio, gravity number and the Dykstra-Parsons coefficient of permeability variation on the performance are investigated. Expressions for pseudo relative permeabilities are also derived. Results .from the developed model were compared with those from conventional models that neglect gravity effecys.

Introduction

The methods available in the literature to predict linear waterflooding performance of stratified reservoirs are grouped into two categories depending on the assumption of communication or no–communication between the different layers. .

In the case of noncommunicating systems, no vertical crossflow is permitted between the adjacent layers.The method of Dykstra–Parsons[1] is the basis for performance prediction in non–communicating stratified reservoirs. Reznik et al.[2] extended the Dykstra-Parsons method to continuous real-time basis.These models assume piston like displacement in the different layers. El-Khatib[3] applied the Bucley-Leverettfrontal advance theory to noncommunicating stratified reservoirs.

A model for communicating stratified reservoirs was presented by Hiatt[4]. This model assumes instantaneous crossflow between layers to keep the pressure gradient the same in all layers at any distance. Warren and Casgrove[5] applied the Hiatt model to a system with log–normal permeability distribution and normal porosity distribution. . El-Khatib[6] presented a closed form analytical solution for communicating stratified systems with log-normal permeability distribution. Hearn[7] used the same model of Hiatt to develop expressions for pseudo relative permeabilities that can be used in numerical reservoir simulation to reduce a 3–dimensional model to a 2–dimensional areal model with average (pseudo) functions for the vertical direction. El–Khatib[8] extended the work of Hiatt to account for variable rock properties other than the absolute permeability and compared performance of communicating and non–communicating systems.

All the mentioned analytical models for prediction of waterflooding performance of stratified reservoirs neglect the effect of density difference between water and oil and thus do not account for vertical crossflow due to gravity..The gravity effect wae ignored to obtain simple analytical solution. In these models, layers are arranged in decreasing order of permeability regardless of their actual location in the reservoir.

However, with sufficient vertical permeability present in a stratified reservoir, the advancing water in a high permeability layer tends to crossflow to the underlying oil zone in a low permeability layer due to the density difference between oil and water. The downward flow of water and upward flow of oil due to phase density difference will delay water breakthrough in high permeability layers and increase oil recovery. The waterflooding performance in this case is expedted to be different from that predicted by models which ignore vertical gravitational crossflow. The actual position of layers in the reservoir will influence the waterflooding performance.

The effect of gravity crossflow on waterflooding performance of stratified reservoirs was investigated experimentally and by means of numerical reservoir simulators. Ahmed, Castanier, and Brigham[9] reported an experimental study for a 2-dimensional layered sand model. Fitzmorris, Kelsey, and Pande[10] investigated the effect of crossflow on sweep efficiency in heterogeneous reservoirs using a 2-dimensional (x-z) fine-grid black oil simulator. Savioli et al.[11] studied the pressure history using finite difference for a radial system of two layers with gravity effects. Tompang and Kelkar[12] compared results from numerical simulation with to results from analytical models of

limiting cases of vertical equilibrium and non-communicating reservoirs. Darman, Sorbie, and Pickup[13] developed transmissibility-poterntial weighted pseudo-functions that better represent gravity-dominated immiscible displacement.

In this work, an analytical model is developed for the performance of waterflooding in communicating stratified reservoirs allowing for vertical gravitational crossflow and maintaining the actual positions of layers in the reservoir.

Theoretical considerations

Vertical Gravity Crossflow

Consider two successive layers i and i+1 with $k_i < k_{i+1}$. At a given time t, the displacement fronts in the two layers are at x_i and x_{i+1} respectively with $x_i < x_{i+1}$ as shown in figure 1-a. For $x<x_i$, water at residual oil saturation is present in both layers. For $x > x_{i+1}$, oil at irreducible water saturation is present in both layers. So in these two zones the same fluid is present in the upper and lower layers and thus gravity does not cause any flow in the vertical direction. For the zone where $x_i < x < x_{i+1}$, the top layer contains oil at irreducible water saturation while the bottom layer contains water at residual oil saturation. In this region, the less dense fluid (oil) lies over the more dense fluid(water) and thus no vertical flow is caused by density difference. The interface between the two layers is considered closed with respect to vertical cross flow and is represented by ——×——

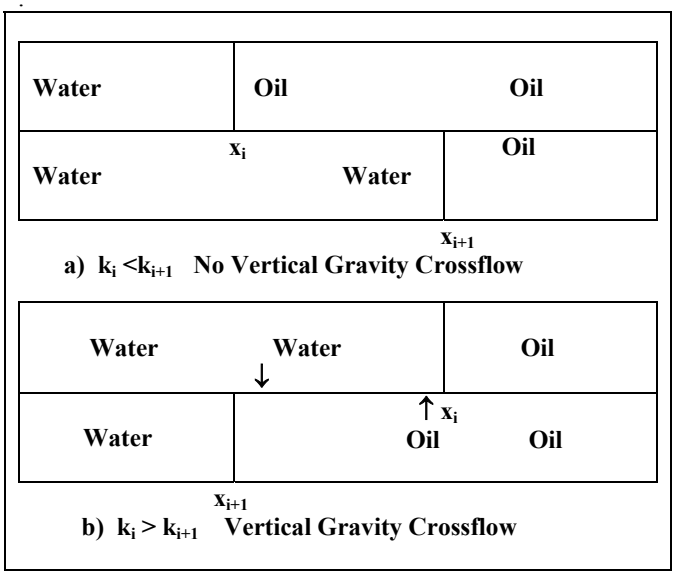

Fig. 1: Conditions for Vertical Gravity Crossflow

Now consider the case for the two successive layers where $k_i > k_{i+1}$ as shown in figure 1-b. At a given time t, the displacement fronts in the two layers are at x_i and x_{i+1} respectively with $x_i > x_{i+1}$. For $x<x_{i+1}$, water at residual oil saturation is present in both layers. For $x > x_i$, oil at irreducible water saturation is present in both layers. So in these two zones, gravity does not cause vertical flow. For the zone where $x_{i+1} < x < x_i$, the top layer contains water at residual oil saturation while the bottom layer contains oil at irreducible water saturation. The density difference between the two fluids will cause flow of water from the upper layer to the lower layer and flow of oil in the opposite direction provided enough vertical communication between the two layers is present. The interface between the two layers is considered open.with respect to vertical cross flow and is represented by ——↓——.

Classification and Grouping of Layers

As discussed earlier, the interface between any two layers is considered close with regard to gravity crossflow if $K_i < K_{i+1}$ and open if $K_i > K_{i+1}$. Any two successive layers with $K_i = K_{i+1}$ are combined into a single layer with the the combined thickness. The upper interface of the first layer and the lower interface of the last layers are considered close.

Accordingly, the layers are classified into four types as shown in figure 2 as follows:

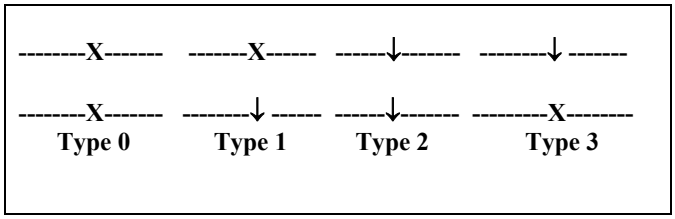

Fig. 2 : Types of Layer w.r.t Gravity Crossflow

1- Type 0, with both the upper and lower interfaces closed
2- Type 1, with the upper the interfac closed and the lower interface open
3- Type 2, with both the upper and lower interfaces open
4- Type 3, with the upper interfac open and the lower interface closed

The first layer of the system is either of type 0 or 1. Type 0 layers are followed by type 0 or 1 and type 1 is followed by type 2 or 3. Type 2 is followed either by type 2 or 3 and type 3 is followed by type 1 or 0. The last layer is of type 0 or 3.

The layers form groups that are classified according to the number of layers in each group. The outer (upper and lower) interfaces of each group are closed while the inner (middle) interfaces are open with respect to gravity crossflow.

Class 1 contains layers of type 0 that are isolated with respect to vertical crossflow. Any group of layers with vertical crossflow between them must have a layer of type 1 at the top and one of type 3 at the bottom. Any intermediate layer in the group must be of type 2. If no intermediate layer is present, the group contains only two layers of types 1-3 and is classified as class 2. If a single layer of type 2 is present between layers 1 and 3, then the group comprises three layers of types 1-2-3 and is classified as class 3. If more than one layer of type 2 is present between layers 1 and 3, then since the solution for a system of more than 3 layers is very complicated, all layers of type 2 in are combined into a single layer with total thickness and average permeability and the system is reduced to class 3 with 3 layers 1-2-3.

Thus the groups of layers are classified into three classes depending on the number of layers in each group as shown in fig. 3..

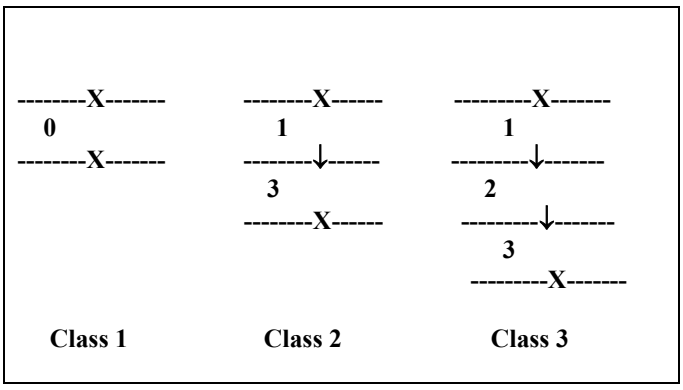

Fig. 3: Classes of layer groups

Mathematical Model

Vertical Crossflow Rate

The flow rates of the two fluids (water and oil) are of equal magnitude and of different directions. The rate can be calculated from Darcy's law and is given by the following equation (see Appendix A)

$$q_v = \frac{K_v \lambda_o^{\circ} \lambda_w^{\circ} \Delta\rho\, gW(x_i - x_{i+1})}{\lambda_t^{\circ}} \quad \ldots\ldots\ldots\ldots\ldots (1)$$

where

K_v = vertical permeability

λ_i = mobility ratio of phase i = K_{ri}/μ_i

$\Delta\rho$ = density difference = $\rho_w - \rho_o$

W = width of layers

Fractional Oil Recovery

The fractional oil recovery (vertical sweep efficiency) at the time of breakthrough in the j^{th} layer, R_j is given by

$$R_j = \frac{1}{h_t}\left[\sum_{\tau_{Bi}\le\tau_{Bj}} \Delta h_i + \sum_{\tau_{Bi}>\tau_{Bj}} X_i \Delta h_i\right] \quad \ldots\ldots\ldots\ldots\ldots (2)$$

For layers of type 0, the location of the front is determined from the equations for the case of no vertical gravity crossflow as given by Hearn[4].

$$X_i = C_i^* \tau_{Bj} = \frac{\tau_{Bj}}{\tau_{Bi}} \quad \ldots\ldots\ldots\ldots\ldots\ldots\ldots\ldots\ldots\ldots (3)$$

$$C_i^* = \frac{dX_i^*}{d\tau} = \frac{\Delta f_{wi}^* h_t}{\Delta h_i \Delta S_w} \quad \ldots\ldots\ldots\ldots\ldots\ldots\ldots\ldots\ldots\ldots (4)$$

$$\tau_{Bi} = 1/C_i^* \quad \ldots\ldots\ldots\ldots\ldots\ldots\ldots\ldots\ldots\ldots (5)$$

For a group of layers of classes 2 (1-3) and 3 or (1-2-3), the location of the displacement fronts are derived in appendix B. However, before the time of breakthrough in the top layer, the following relation could be used for the purpose of calculating oil recovery.

$$\sum X_i \Delta h_i = \sum X_i^* \Delta h_i \quad \ldots\ldots\ldots\ldots\ldots\ldots\ldots (6)$$

Calculation of Water Cut f_w

At any timeτ, all layers with $\tau_B \le \tau$ are producing water at the outlet end of the system while those layers with $\tau_B > \tau$ are producing oil. Layers of type 1or 2 that producing water will transfer a rate q_v to the layers lying beneath them of types 2 or 3 untill these layers reach breakthrough. This vertical crossflow due to gravity will reduce the water cut f_w below its value f_w^* calculated without gravity effect which is given by

$$f_{wj}^* = \frac{Mc_j}{Mc_j + (c_t - c_j)} \quad \ldots\ldots\ldots\ldots\ldots\ldots\ldots\ldots (7)$$

From material balance considerations

$$q_{wj} = f_{wj}^* q_t - \sum q_v \quad \ldots\ldots\ldots\ldots\ldots\ldots\ldots\ldots\ldots (8)$$

So

$$f_{wj} = \frac{q_{wj}}{q_t} = f_{wj}^* - \frac{\sum q_v}{q_t} \quad \ldots\ldots\ldots\ldots\ldots\ldots\ldots\ldots (9)$$

For a group of layers of class 2 or 3 before B.T. in the second layer, q_v is given by Eq. (1) with $x_i = L$.

$$\frac{q_v}{q_t} = \frac{N_G}{(1+M)}(1 - X_{i+1}) \quad \ldots\ldots\ldots\ldots\ldots\ldots\ldots (10)$$

and for a class 3 after B.T. in the middle layer

$$\frac{q_v}{q_t} = \frac{N_G}{(1+M)}(1 - X_{i+2}) \quad \ldots\ldots\ldots\ldots\ldots\ldots\ldots (11)$$

The dimensionless Gravity number N_G is defined as

$$N_G = \frac{K_v \lambda_o^{\circ}\ \Delta\rho\, gLW}{q_t} \quad \ldots\ldots\ldots\ldots\ldots\ldots\ldots\ldots (12)$$

where X_{i+1} is given by Eq. (B-12) for 2-layer case and Eq. (B-24) for 3-layer case while X_{i+2} is given by Eq. (B-31). Terms of q_v/q_t should be added for all groups of classes 2 and 3 for which the top layer passed B.T. time while at least one of the remaining layers did not reach B.T. time.

Pseudo-Relative Permeability Functions

For the case of no gravity effect

$$q_w^* = q_t f_w^* = \frac{\overline{K}\widetilde{K}_{rw}^* W h_t}{\mu_w}\left(-\frac{dp}{dx}\right) \quad \ldots\ldots\ldots\ldots\ldots (13)$$

and when gravity effect is considered

$$q_w = q_t f_w = \frac{\overline{K}\widetilde{K}_{rw} W h_t}{\mu_w}\left(-\frac{dp}{dx}\right) \quad \ldots\ldots\ldots\ldots\ldots\ldots (14)$$

From Eq. (13) and (14)

$$\widetilde{K}_{rw} = \widetilde{K}_{rw}^* \frac{f_w}{f_w^*} \quad \ldots\ldots\ldots\ldots\ldots\ldots\ldots\ldots (15)$$

Similarly

$$\widetilde{K}_{ro} = \widetilde{K}_{ro}^* \frac{(1-f_w)}{(1-f_w^*)} \quad \ldots\ldots\ldots\ldots\ldots\ldots\ldots\ldots (16)$$

where

$$\widetilde{K}^{*}_{rwj} = K^{\circ}_{rw}\frac{c_j}{c_t} \quad \text{..... (17)}$$

and

$$\widetilde{K}^{*}_{roj} = K^{\circ}_{ro}(1-\frac{c_j}{c_t}) \quad \text{..... (18)}$$

The water saturation corresponding to these pseudo-relative permeabilities is given by

$$\widetilde{S}_{wj} = S_{wi} + \Delta S_w \sum_{\tau_{Bi}\le\tau_{Bj}} \Delta h_i / h_t \quad \text{..... (19)}$$

Solution Procedure

The algorithm used for computations performs the following main steps

1- Classification, Combination and Grouping of Layers

The data for the different layers as obtained from cores, logs or geostatistical models are entered according to their location in the reservoir. Any two or more successive layers with the same permeability are combined into a single layer with the total thickness of the combined layers.

The interfaces between the different layers are classified as open or closed depending on the absolute permeabilities of the layers on each side of the interface. The upper interface of the first layer and the lower interface of the last layers are considered close.The layers are then classified into four types according to their top and bottom interfaces. The layers are then separated into groups of different classes depending on the number of layers in each group..

2-Calculations for the no-gravity case

Since these values are needed in the model equations we start by determining the system's performance neglecting gravity effects using Hearn's method[7].

The layers are arranged in decreasing order of permeability and the formation capacity c_j is calculated for each layer. The fractional flow f_w is calculated for each layer using Eq. (7).The frontal advance $dX^*/d\tau$ is calculated using Eq. (4).The time of B.T for each layer is calculated using Eq. (5).The fractional oil recovery is calculated from the equation

The pseudo relative perrmeabilities for water and oil are calculated using Eq. (17) – (18).

$$R_j = \frac{h_j}{h_t} + \frac{(1-f^*_{wj})}{\Delta f^*_{wj}}\Delta h_j \quad \text{..... (20)}$$

3-Determination of B.T. time with gravity effects

Layers are taken in the order of their location in the reservoirs.

For layers of type 0, the B.T. time is the same as that calculated neglecting gravity effects, Eq. (5)..

For layers of class 2 which consist of two layers of sequence 1-3, Eq. (B-10) is solved iteratively for B.T. time of the top layer by setting $X_i = 1$. The time of B.T in the bottom layer is calculated from Eq. (B-13)).

For layers of class 3 which consist of three layers of sequence 1-2-3, Eq. (B-17) is solved iteratively for B.T. time of the top layer by setting $X_i = 1$. The locations of the fronts in the middle and bottom layers at the time of B.T in the top layer are determined from Eq. (B-18) and (B-19). Eq. (B-24) is then solved iteratively for B.T. time of the middle layer by setting $X_{i+1} = 1$. The location of the front in the bottom layer at the time of B.T in the middle layer is determined from Eq. (B-25). The time of B.T in the bottom layer is then calculated using Eq. (B-32).

This procedure is repeated until the last group of layers is reached

4- Determination of Fractional Oil Rcovery R_j and Water Cut f_w

At the time of breakthrough in the j^{th} layer, starting from j=1 to j=n, the fractional oil recovery R_j (vertical sweep efficiency) is calculated using Eq.(2) . .

To determine the front locations for layers with $\tau_{Bi} > \tau_{Bj}$, the following procedure is followed. (X=1 for $\tau_{Bi} > \tau_{Bj}$)

For layers of type 0, the location of the front is determined by Eq. (3).

For a group of layers of class 2 or 3 if the top layer did not reach its time of B.T., the locations of the fronts in the case of no gravity is used for calculating fractional recovery purposes because of the validity of Eq. (6).

For a group of class 2 layers with the top layer after B.T and the bottom layer before B.T., Eq.(B-11) is used to calculate the location X_L of the front in the bottom layer at time of B.T. in the top layer τ_{Bi} , then Eq. (B-12)) is used to calculate the location X_{i+1} at τ_{Bj}. Equation (10) is used to calculate q_v/q_t.

For a group of class 3 layers with the top layer after B.T and the middle and bottom layers are before B.T., Eq.(B-18) and (B-19) are used to calculate the locations of the fronts in the middle and bottom layers at time of B.T. in the top layer τ_{Bi} , then Eq. (B-24) and (B-25) are used to calculate the locations X_{i+1} and X_{i+2} at τ_{Bj}. Equation (10) is used to calculate q_v/q_t.

For a group of class 3 layers with the top and middle layers are after B.T and the bottom layer is before B.T., Eq.(B-25) is used to calculate the locations of the front X_{3LL} in the bottom layers at time of B.T. in the middle layer τ_{Bi+1} , then Eq. (B-31) is used to calculate the location X_{i+2} at τ_{Bj}. Equation (11) is then used to calculate q_v/q_t.

This procedure is repeated until the last group of layers is reached.

The values of q_v/q_t from all layers are added and Eq. (9) is used to calculate the water cut f_{wj}.

5- Calculation of the pseudo-relative Permeability Curves

Equations (15) and (16) are used to calculate the pseudo relative permeabilities for oil and water respectively at the corresponding water saturation given by Eq. (19).

6- Ordering of Results

After calculations are performed for all layers in the order of their location in the reservoir, the results are sorted in an increasing order of time and recovery.

Results and Discussion

Usually, the permeability has a log–normal distribution. With

$$p(k) = .5 + .5erf\left[\frac{\ln(k/k_m)}{\sqrt{2}\sigma_k}\right] \quad \text{..... (21)}$$

The heterogeneity of the reservoir is described by means of the standard deviation of the permeability distribution σ_k. Another commonly used measure is the Dykstra-Parsons coefficient of variation V_{DP}. V_{DP} is related to σ_k by the relation $\sigma_k = \ln [1 / (1 - V_{DP})]$

A value of V_{DP} of 0 represents a homogeneous reservoir (constat K) while a value of 1 represents a totally heterogeneous reservoir.

Effect of Gravity Number

The developed method was applied to a hypothetical stratified reservoir of 20 layers with permeability generated from a log-normal distribution with V_{DP} =.5. A mobility ratio of 2 was used. The porosity and end point relative permeabilities are assumed the same for all layers. Results were obtained for values of the Gravity number N_G of 0.1, 1, 10. Results for N_G of 0 are obtained as part of the solution for all cases.

Figure 4 shows the fractional oil recovery R as function of dimensinless time τ. It is clear that the oil recovery is higher for the gravity case than for the case when gravity crossflow is ignored. The recovery increases as N_G increases from 0.1 to 1, but little increase is shown when N_G is increased from 1 to 10, At late times when R approaches unity (ultimate recoverable oil), all curves ccooncide. This corresponds to water breakthrough in most of the layers.

Figure 5 shows the water cut f_w vs. dimensionless time τ. The results indicate delayed water breakthrough and lower water cut as the Gravity number N_G increases. Again the effect

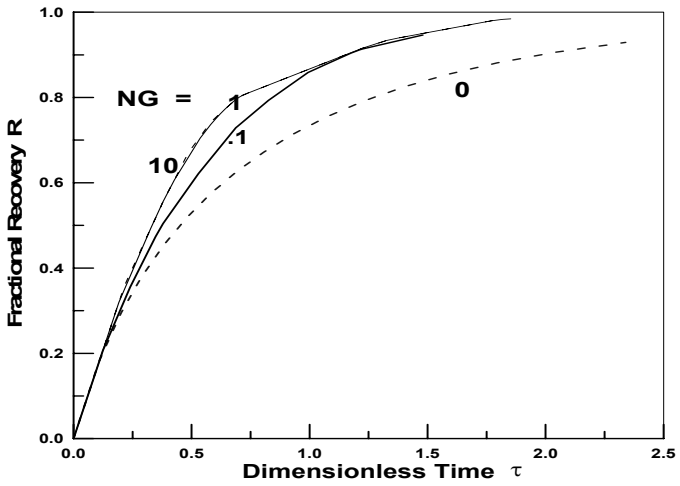

Fig. 4: Effect of Gravity Number on Performance, *R* vs. τ

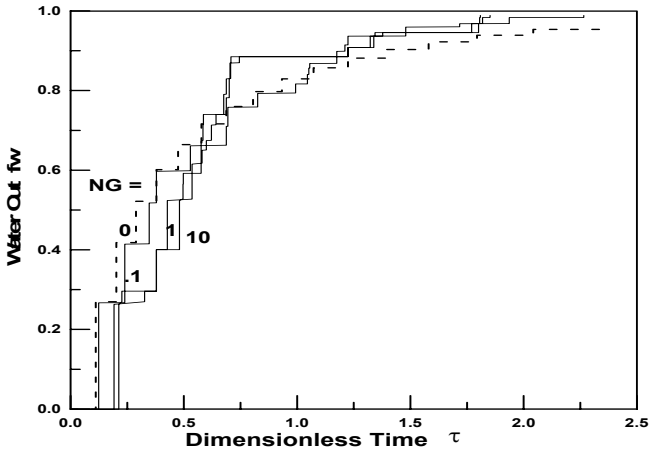

Fig. 5: Effect of Gravity Number on Performance, f_w vs. τ

is apparent when N_G increases from 0.1 to 1 and less remarkablewhen N_G increases from 0.1 to 1. It is to be noticed that the water cut in the no gravity case at the times of water breakthrough in the successive layers and not at the absolute value ofdimensionless time. This behavior is better shown in Fig. 6 where the water cut f_w is plotted vs. the fractional oil recovery R. It is clear that gravity crossflow results in delayed water breakthrough, higher oil recovery and lower water cut. This effect increases as the Gravity number N_G increases. Also the difference in performances for N_G of 0.1 and 1 is more remarkable than that for N_G of 1 and 10 .

These results are expected since vertical crossflow caused by gravity forces moves water downwards from higher to lower permeability layers. This will cause delaying the water breakthrough in the higher permeability layers and sharpening the displacement profile resulting in higher oil recovery.

Figure 7 is a plot of oil and water pseudo relative permeability curves. The results indicate that gravitational crossflow causes increase of the oil and decrease in the water pseudo relative permeabilities as compared to the case with no gravitational crossflow. This will result in the fractional flow curves to be lower for the crossflow case as shown in fig. 8. Increasing the Gravity number will increase this effect since vertical crossflow is proportional to the Gravity number.

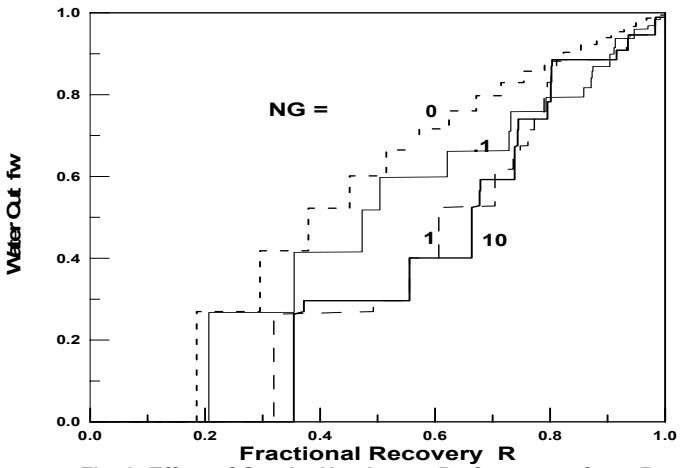

Fig. 6: Effect of Gravity Number on Performance, f_w vs. *R*

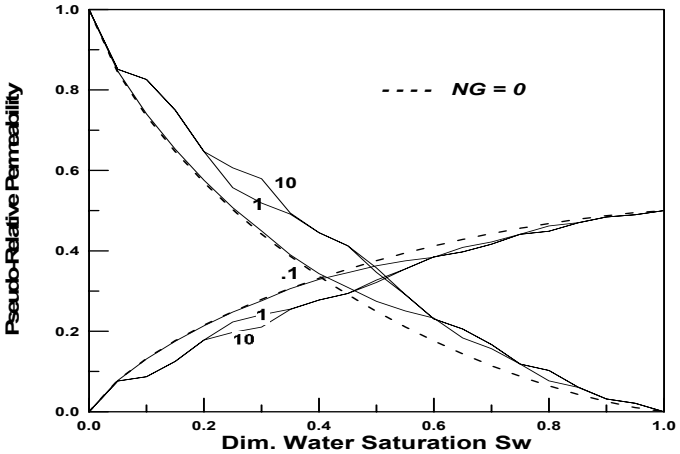

Fig. 7: Effect of Gravity Number on Pseudo Rel. Permebility

Effect of Mobility Ratio

Results were obtained for values of the mobility ratio of .5, 1, 5. The gravity number was 1 for all cases.Figure 9 shows the performance in terms of water cut f_w vs. fractional oil recovery *R*. The recovery decreases and the water cut increases for higher (unfavorable) mobility ratios. For all mobility ratios, the oil recovery is higher and the water cut is lower when vertical gravity crossflow is taken into consideration. This effect is more pronounced for high (unfavorable) mobility ratios. This is because for the case of high mobility ratios, the displacement front is very diffused and vertical crossflow will sharpen the front and thus remarkably delay the water breakthrough and increase oil recvery. For favorable mobility ratios, the displacement front is already sharp and taking vertical crossflow into consideration will not improve it too much.

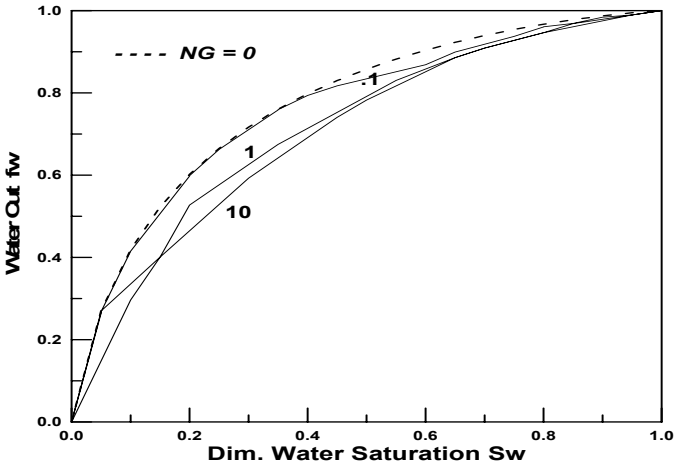

Fig. 8: Effect of Gravity Number on Fractional Flow Curves

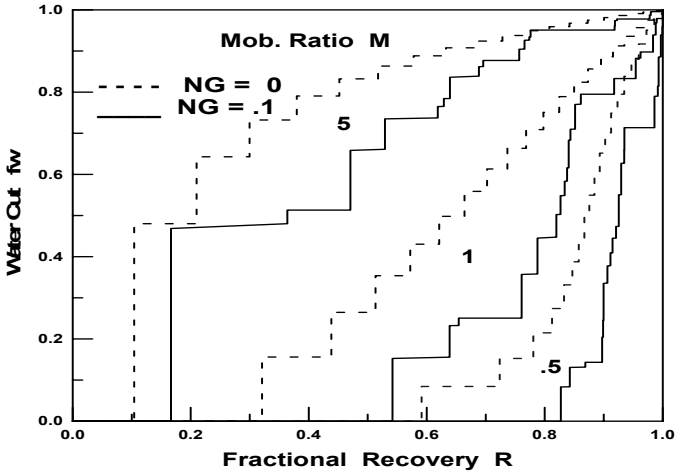

Fig. 9: Effect of Mobility Ratio *M* on Performance

Figure 10 shows the pseudo relative permeability curves for the different mobility ratios. It is known that when gravity effect is ignored, the mobility ratio has no effect on the pseudo relative permeabilities as indicated by Eq. ( ),( ). Vertical crossflow will affect the pseudo curves as shown by EQ. ( )-( ). Although the effect of the mobility ratio on the pseudo relative permeabilities seems to be small, this effect is more pronounced for high (unfavorable) mobility ratios.

Effect of Permeability Variation

To investigate the effect of reservoir heterogeneity, permeability distributions were sampled from a log-normal distribution with values of V_{DP} of 01, .3, .7 and .9..

Figure 11 shows the fractional oil recovery vs. dimensionless time while fig. 12 shows the water cut f_w vs. oil recovery. The fractional oil recovery decreases and the water cut increases as the variation coefficient V_{DP} increases from 0.1 to 0.9. Gravitational crossflow tends to remedy the effect of heterogeneity by sharpening the displacement front. This is seen in fig. 11 for the case of V_{DP} of 09.

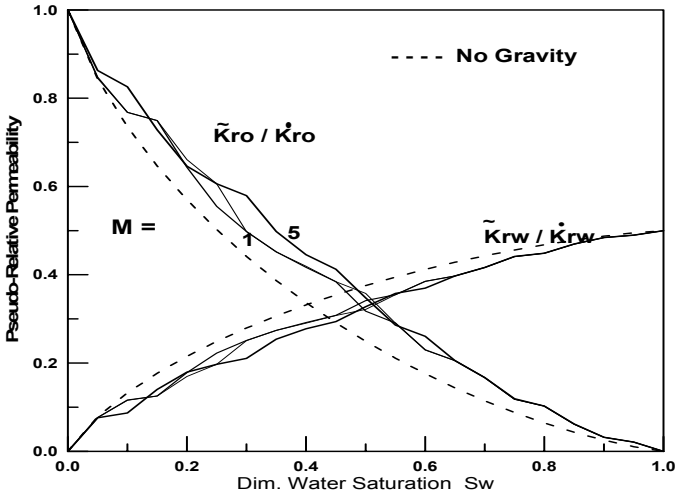

Fig. 10: Effect of Moblity Ratio on Pseudo Rel. Permebility

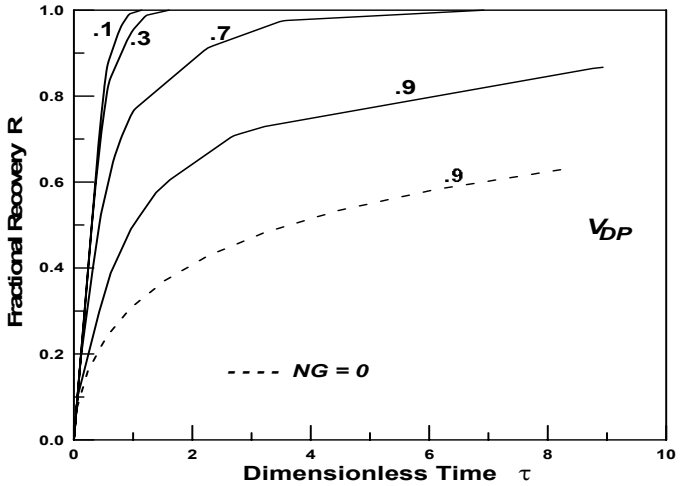

Fig. 11: Effect of Heterogeneity on Performance. R vs. τ

Figure 13 shows the effect of reservoir heterogeneity on the pseudo relative permeability curves. More heterogeneous reservoirs (high V_{DP}) have lower oil and higher water pseudo relative permeabilities as compared to more homogeneous (low V_{DP}) reservoirs. As expected, gravity forces increase the oil and reduce the water pseudo relative permeabilities for the same V_{DP} value.

Effect of Layers Ordering (Randomness)

Since gravitational crossflow depends on the actual location of the different layers in the reservoir, layer ordering is expected to have a marked effect on waterflooding performance. To investigate this effect, 10 different realizations were generated from a log normal permeability distribution with the same mean and standard deviation (V_{DP}=0.5). Figure 14 shows the different permeability distributions.. Results were obtained for the different realizations for N_G= 1 and M= 2. and are shown in figures 15 – 18. The case with no gravity effect (N_G= 1 is also shown in these figures.

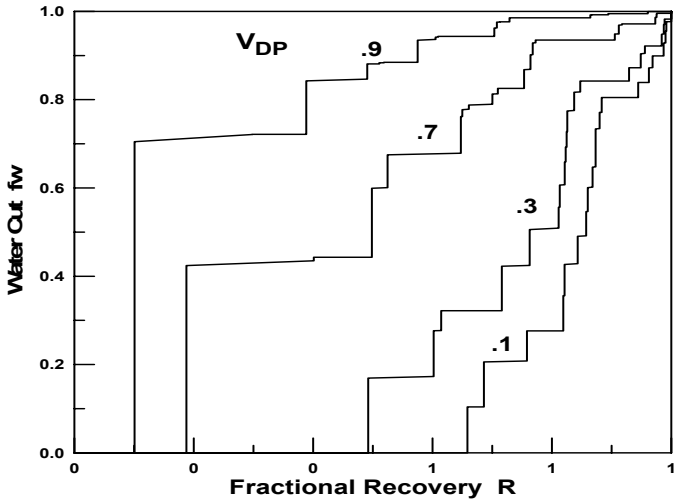

Fig. 12: Effect of Heterogeneity on Performance. F_w vs. R

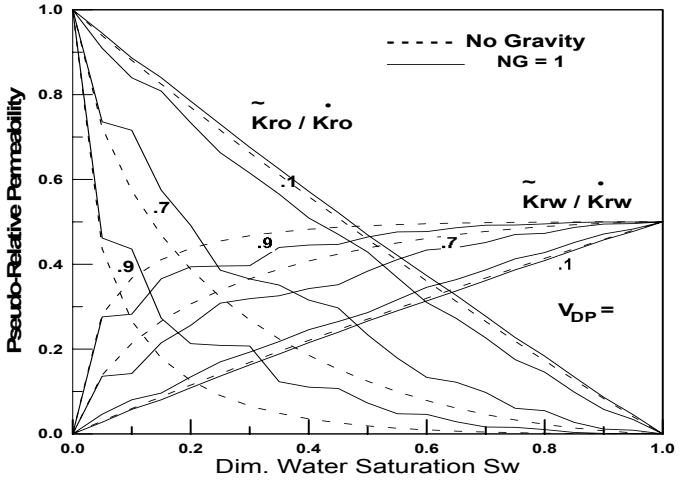

Fig. 13: Effect of Heterogeneity on Pseudo Rel. Permeabilty

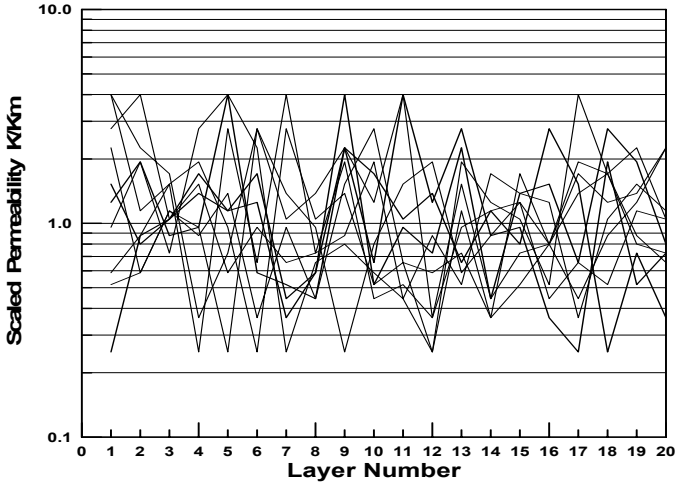

Fig. 14: Random permeability Distributions – 10 Realizations

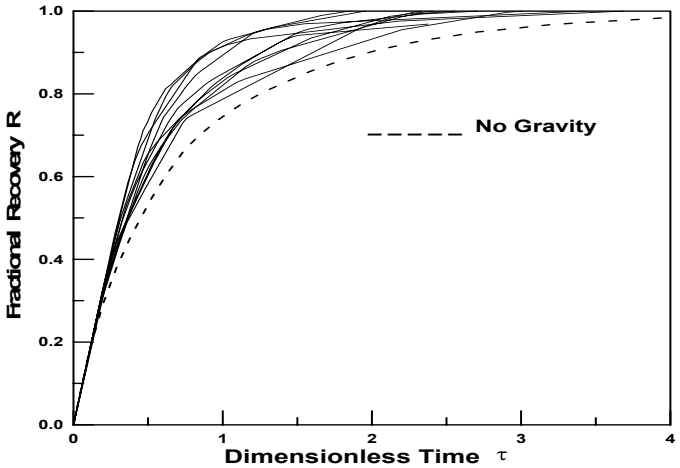

Fig. 15: Performance for Different Random Distributions, *R* vs. τ

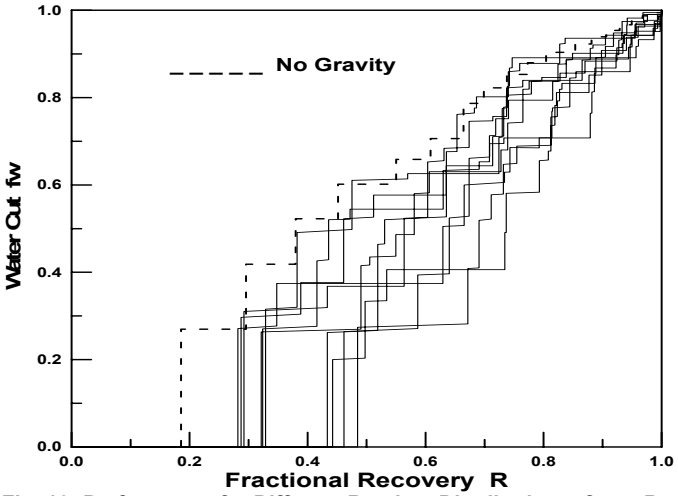

Fig. 16: Performance for Different Random Distributions, f_w vs. R

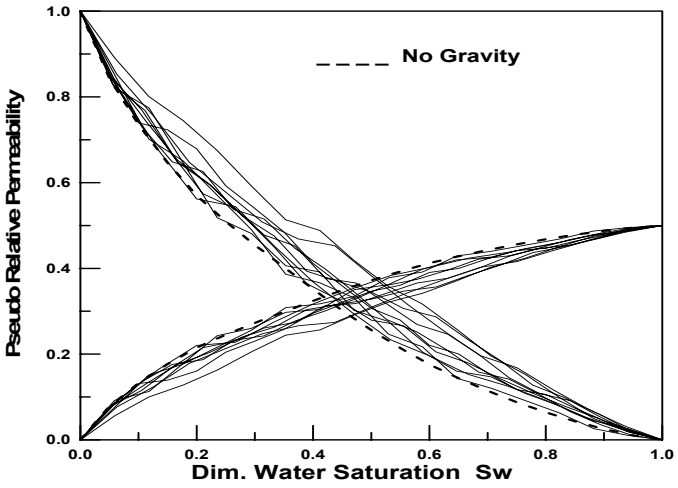

Fig. 17: Pseudo Relative Permeability Curves for Different Random Permeability Distributions

The results show a wide variation of the performance which indicates the relevance of layers locations on the performance of waterflooding of vertically communicated stratified reservoirs. The variations in the performance for the different realizations begin after water breakthrough in the most permeable layers occur. Before that, Eq. ( ) implies the performance wuld be independent of gravitational cross flow

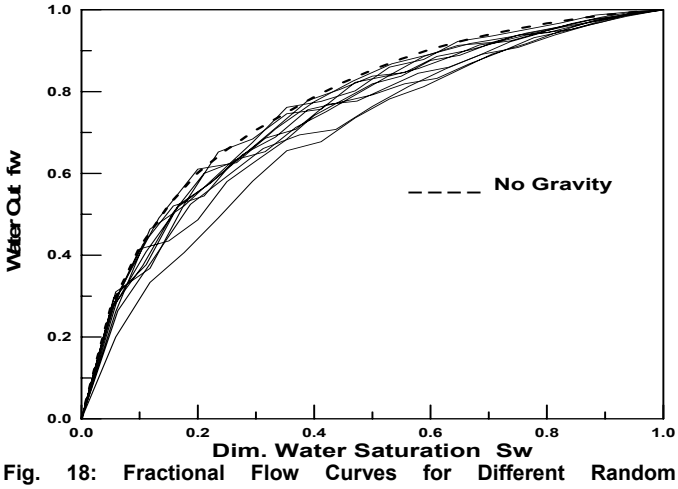

Fig. 18: Fractional Flow Curves for Different Random Permeability Distributions

Conclusions

1- A mathematical model was developed for waterflooding of communicating stratified reservoirs considering the vertical gravitational crossflow caused by density difference of oil and water. The cornerstone of the model is the derivation and solution of the system of differential equations describing the movement of the displacement fronts in the different layers. These solutions are used to estimate fractional oil recovery, water cut and pseudo relative permeability curves

2- A solution procedure is developed to calculate the waterflooding performance of stratified reservoirs with vertical gravitational crossflow. The procedure involves classification of layers with respect to gravitational cross flow and grouping the layers into classes depending on their relative locations.

3- The results show that gravitational crossflow delays waterbreakthrough in high permeablity layers, increases oil recovery and decreases water cut. The influence of gravitational crossflow increases with Gravity number until a value of 1 after which the change in performance becomes small.

4- The effect of gravitational crossflow on the performance is more evident for the cases of unfavorable mobility ratios and for cases of highly heterogeneous reservoirs ($V_{DP}\approx 1$).

5- The order of layer permeability distribution in the reservoir has a large effect on the waterflooding performance of stratified reservoirs with gravity effects. This implies that the layers should be placed in their actual location with respect to each other for accurate modeling of the system.

Nomenclature

A = area, L^2, ft^2 [m^2]
C = formation capacity, L^3, md.ft [μm^3]
f_w = fractional flow of water, dimensionless
h_t = total formation thickness, L, ft [m]
g = acceleration og gravity, L/t^2. ft/sec^2 [m/sec^2]
k = absolute horizontal permeability, L^2, md [μm^2]
k_m = mean permeability distribution, L^2, md [μm^2]

k_{ro}^{o} = oil relative permeability at irreducible water saturation, dimensionless
$\tilde{k}_{ro}$ = pseudo relative permeability for oil, dimensionless
k_{rw}^{o} = water relative permeability at residual oil saturation, dimensionless
$\tilde{k}_{rw}$ = pseudo relative permeability for water, dimensionless
L = length, L, ft [m]
M = mobility ratio, dimensionless
N_G = Gravity number, dimensionless
P = pressure
$P(k)$ = distribution function of permeability, dimensionless
q = flow rate, L^3/t , bbl/d [m^3/s]
R = vertical coverage, dimensionless
S_D = dimensionless water saturation
Sor = residual oil saturation, fraction
Sw = water saturation, fraction
Swi = initial water saturation, fraction
ΔS_w = displaceable oil saturation, fraction
t = time, t, d [s]
V_{DP} = Dykstra–Parsons variation coefficient, dimensionless
x = distance of displacement front
X = dimensionless distance of the displacement front
μ = viscosity, m/Lt, cp.[Pa.s]
σ_k = standard deviation of P(k)
λ = mobility = K/μ , L3t/ m , md/cp [m2/Pa.s]
μ = viscosity, m/Lt, cp [Pa.s]
ϕ = porosity, fraction
τ = dimensionless time

Subscripts

B = Breakthrough
I = initial , irreducible
k = permeability
m = mean
o = oil
t = total
v = vertical
w = water

Superscripts

O = end point
* = no gravity case

Acknowledgement

The author wishes to acknowledge the support provided by the Petroleum Engineering Department of King Saud University during this study.

References

1. Dykstra, H. and parsons, R.L.: "The Prediction of Oil recovery by Waterflooding," Secondary Recovery of Oil in the United States, 2nd ed., API (1950) 160–174.
2. Reznik, A.A., Enick, R.M. and Panvelker, S.B.: "An Analytical Extension of the Dykstra–Parsons Vertical Stratification Discrete Solution to a Continuous, Real–Time Basis," *Soc. Pet. Eng. J.* (1984) **24**, 643–656.
3. El–Khatib, N.A.: "The Application of Buckley-Leverett Displacement to Waterflooding in Non-Communicating Stratified Reservsoirs," paper SPE 68076 presented at 2001 SPE Middle East Oil Show, Bahrain, March 17-20.
4. Hiatt, N.W.: "Injected–fluid Coverage of Multi–well Reservoirs with Permeability Stratification," Drill and Prod. Prac., API (1958) 165, 165–194.
5. Warren, J.E. and Cosgrove, J.J.: "Prediction of Waterflood Behavior in a Stratified System," *SPEJ*. (June 1964) 149–157.
6. El–Khatib, N.A.: "Waterflooding Performance of communicating Stratified Reservsoirs with Log-Normal Permeability Distribution," *SPEREE* , (Dec. 1999), 542.
7. Hearn, C.L.: "Simulation of Stratified Waterflooding by Pseudo Relative Permeability Curves," *J. Pet. Tech.* (July 1971), 805–813.
8. El–Khatib, N.A.: "The Effect of Crossflow on Waterflooding of Stratified Reservsoirs," *Soc. Pet. Eng. J.* (April, 1985), 291–302.
9. Ahmed, G., Castanier, L.M., and Brigham, W.E.:"An Experimental Study of Waterflooding from a Two-Dimensional Layered Sand Model," *SPERE*, (Feb. 1988), 45.
10. Fitzmorris, R.E., Kelsey, F.J., and Pande, K.K.: "Effect of Crossflow on Sweep Efficiency in Water/Oil Displacements in Heterogeneous Reservoirs," paper SPE 24901 presented at the 1992 Annual Technical Conference and Exhibition, Washington, D.C., Oct. 4-7.
11. Savioli, G.B., et al.: "Pressure Response of Layered Reservoirs with Crossflow in the Presence of Gravity Effects," paper SPE 53930 presented at the 1999 SPE Latin American and Caribbean Petroleum Engineering Conference, Caracas, Venezuela, April 21-23.
12. Tompang, R., and Kelkar, B.G.: "Prediction of Waterflood Performance in Stratified Reservoirs," paper SPE 17289 presented at the 1988 SPE Permian Basin Oil and Gas Recovery Conference, Midland, Texas, March 10-11.
13. Darman, N.H., Sorbie, K.S., and Pickup, G.E.: "The Development of Pseudo Functions for Gravity-Dominated Immiscible Gas Displacements," paper SPE 51941 presented at the 1999 SPE Reservoir Simulation Conference, Houston, Texas, Feb. 14-17.

Appendix A: Derivation of Gravitational Crossflow Equation

Since the net flow of oil and gas in the vertical direction is zero, then from Darcy law where the +ive z-direction is taken as the downward vertical direction.

$$-1.127K_v\left[\lambda_w^{\circ}\left(\frac{dP}{dz}-.433\rho_w\right)+\lambda_o^{\circ}\left(\frac{dP}{dz}-.433\rho_o\right)\right]=0 \quad \text{..... (A-1)}$$

From which

$$\frac{dP}{dz} = \frac{.433(\rho_w \lambda_w^\circ + \rho_o \lambda_o^\circ)}{(\lambda_w^\circ + \lambda_o^\circ)} \quad \text{..... (A-2)}$$

Using this pressure gradient in Darcy equation for the water phase and reaaranging

$$q_{wv} = \frac{.488 K_v A \Delta\rho \lambda_w^\circ \lambda_o^\circ}{\lambda_t} \quad \text{..... (A-3)}$$

Appendix B: Frontal Advance and Front Locations with Gravity Effects

Two layer case.

For the case of two layers with $K_i > K_{i+1}$ as shown in fig.B-1, the vertical crossflow will cause a retreat of the front in the i^{th} layer from x_i^* to x_i with

$$q_v = w\Delta h_i \varphi_i \Delta S_{wi} \frac{d}{dt}(x_i^* - x_i) \quad \text{..... (B-1)}$$

The same crossflow will cause an advance of the front in the $i+1^{st}$ layer from x_{i+1}^* to x_{i+1} with

$$q_v = w\Delta h_{i+1} \varphi_{i+1} \Delta S_{i+1} \frac{d}{dt}(x_{i+1} - x_{i+1}^*) \quad \text{..... (B-2)}$$

where

Δh = layer thickness

ϕ = porosity

$\Delta S_w = 1 - S_{wi} - S_{or}$

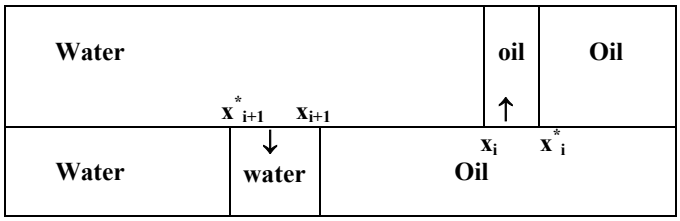

Fig. B-1: Front Location Relations in two-layer case

Substituting Eq. (A-3) for q_v with the crossflow area between the two layers is $L(X_i - X_{i+1})$ and using dimensionless variables we get

$$\frac{dX_i}{d\tau} + \alpha_i (X_i - X_{i+1}) = C_i^* \quad \text{..... (B-3)}$$

and

$$\frac{dX_{i+1}}{d\tau} - \alpha_{i+1} (X_i - X_{i+1}) = C_{i+1}^* \quad \text{..... (B-4)}$$

where

$$X = x/L \quad \text{..... (B-5)}$$

$$\tau = \frac{\int_0^t q_t dz}{W h_t \varphi L} \quad \text{..... (B-6)}$$

$$\alpha_i = \frac{N_G}{(1+M)} \frac{h_t}{\Delta h_i \Delta S_w} \quad \text{..... (B-7)}$$

$$N_G = \frac{K_v \lambda_o^\circ \Delta\rho \, gLW}{q_t} \quad \text{..... (B-8)}$$

$$C_i^* = \frac{dX_i^*}{d\tau} = \frac{\Delta f_{wi}^* h_t}{\Delta h_i \Delta S_w} \quad \text{..... (B-9)}$$

Eqations (B-3) and (B-4) represent a system of two simultaneous ordinary nonhomogeneous linear differential equations with constant coefficients.

The solution of this system of equations is given by

$$X_i = C_i^* \tau - \frac{\alpha_i (C_i - C_{i+1})}{\alpha_i + \alpha_{i1}} \left[\tau - \frac{1 - e^{-(\alpha_i + \alpha_{i1})\tau}}{\alpha_i + \alpha_{i1}} \right] \quad \text{(B-10)}$$

$$X_{i+1} = C_{i+1}^* \tau + \frac{\alpha_{+1i} (C_i - C_{i+1})}{\alpha_i + \alpha_{i1}} \left[\tau - \frac{1 - e^{-(\alpha_i + \alpha_{i1})\tau}}{\alpha_i + \alpha_{i1}} \right]$$

..... (B-11)

Equations (B-10) and (B-11) are valid before waterbreakthrough in the upper layer, $X_i \le 1$. After waterbreakthrough in the i^{th} layer, X_i=1 is substituted in Equation (B-4) which now has the solution

$$X_{i+1} = (X_L - 1 - \frac{C^*_{i+1}}{\alpha_{i+1}}) e^{-\alpha_{i+1}(\tau - \tau_{Bi})} + 1 - \frac{C^*_{i+1}}{\alpha_{i+1}} \quad \text{... (B-12)}$$

where τ_{Bi} is the time of water breakthrough in the i^{th} layer and is obtained by solving Eq. (B-10) for X_i=1 iteratively and X_L is the location of the displacement front in the $i+1^{st}$ layer at the time of water breakthrough in the i^{th} layer and is obtained by setting $\tau = \tau_{Bi}$ in Eq.(B-11) . Setting X_{i+1} = 1, Eq. (B-12) can be solved for the time of water breakthrough in the $i+1^{st}$ layer

$$\tau_{Bi+1} = \tau_{Bi} + \frac{1}{\alpha_{i+1}} \ln \left[1 + \frac{(1 - X_L)}{C^*_{i+1}} \alpha_{i+1} \right] \quad \text{..... (B-13)}$$

Three layer case.

For the case of three successive layers i, i+1 and i+1 with $K_i > K_{i+1} > K_{i+2}$ (Fig. B-2), downward flow of water and upward flow of oil take place between the three layers. The top layer looses water and gains oil while the opposite happens for the bottom layer. The conditions in the middle layer will depend of the relative amounts of fluids entering and leaving the layer.

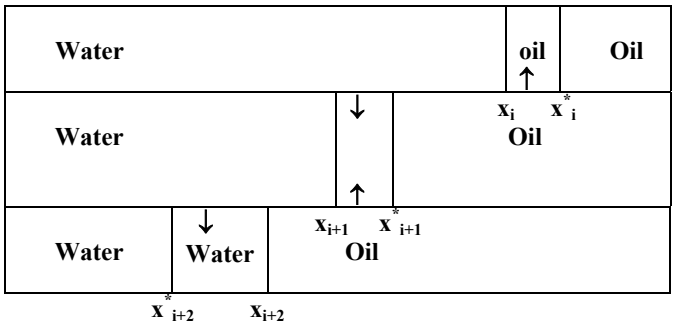

Fig. B-2: Front Location Relations in three-layer case

The system of differential equations describing mass conservation in the three layers is given by

$$\frac{dX_i}{d\tau}+\alpha_i(X_i-X_{i+1})=C_i^* \quad \text{(B-14)}$$

$$\frac{dX_{i+1}}{d\tau}-\alpha_{i+1}(X_i-X_{i+1})+\alpha_{i+1}(X_{i+1}-X_{i+2})=C_{i+1}^* \quad \text{(B-15)}$$

and

$$\frac{dX_{i+2}}{d\tau}-\alpha_{i+2}(X_{i+1}-X_{i+2})=C_{i+2}^* \quad \text{(B-16)}$$

The solution for this system of equations is

$$X_i=C_i^*\tau-\frac{\alpha_i(C_i^*-C_{i+1}^*)}{ab}(1-S_1)-\frac{\alpha_i\left[\alpha_{i+1}(C_i^*-C_{i+2}^*)+\alpha_{i+2}(C_i^*-C_{i+1}^*)\right]}{ab}\left[\tau-\frac{a+b}{ab}+S_2\right] \quad \text{(B-17)}$$

$$X_{i+1}=C_{i+1}^*\tau-\frac{\alpha_{i+1}(C_i^*-2C_{i+1}^*+C_{i+2}^*)}{ab}(1-S_1)+\frac{\alpha_{i+1}\left[\alpha_{i+2}(C_i^*-C_{i+1}^*)-\alpha_i(C_{i+1}^*-C_{i+2}^*)\right]}{ab}\left[\tau-\frac{a+b}{ab}+S_2\right] \quad \text{(B-18)}$$

$$X_{i+2}=C_{i+2}^*\tau+\frac{\alpha_{i+2}(C_{+1i}^*-C_{i+2}^*)}{ab}(1-S_1)-\frac{\alpha_{i+2}\left[\alpha_i(C_{i+1}^*-C_{i+2}^*)+\alpha_{i+1}(C_i^*-C_{i+2}^*)\right]}{ab}\left[\tau-\frac{a+b}{ab}+S_2\right] \quad \text{(B-19)}$$

Where

$$S_1=\frac{be^{-a\tau}-ae^{-b\tau}}{b-a} \quad \text{(B-20)}$$

$$S_2=\frac{b^2e^{-a\tau}-a^2e^{-b\tau}}{ab(b-a)} \quad \text{(B-21)}$$

$$a=\frac{\alpha_i+2\alpha_{i+1}+\alpha_{i+2}}{2}+.5\sqrt{(\alpha_i-\alpha_{i+2})^2+4\alpha_{i+1}^2} \quad \text{(B-22)}$$

$$b=\frac{\alpha_i+2\alpha_{i+1}+\alpha_{i+2}}{2}-.5\sqrt{(\alpha_i-\alpha_{i+2})^2+4\alpha_{i+1}^2} \quad \text{(B-23)}$$

The time of breakthrough in the upper layer τ_{Bi} is obtained by solving Eq. (B-17) for $X_i = 1$. The location X_{2L} and X_{3L} of the fronts in the other two layers are obtained by substituting this time in Eq. (B-18) and (B-19) respectively. For $\tau > \tau_{Bi}$, X_i in Eq. (B-15) is replaced by 1 and the solution for the system o Eq. (B-15) and (B-16) is given by

$$X_{i+1}=\frac{(\alpha_{i+1}+C_2^*)+\alpha_{i+2}X_{2L}+\alpha_{i+1}X_{3L}}{b-a}S_3-\frac{X_{3L}}{b-a}S_4+\frac{\alpha_{i+1}\alpha_{i+2}+\alpha_{i+2}C_2^*+\alpha_{i+1}C_3^*}{a_1b_1}(1-S_5) \quad \text{(B-24)}$$

$$X_{i+2}=\frac{C_2^*+\alpha_{i+2}X_{2L}+2\alpha_{i+1}X_{3L}}{b_1-a_1}S_3-\frac{X_{3L}}{b-a}S_4+\frac{\alpha_1\alpha_{i+2}+\alpha_{i+2}C_2^*+2\alpha_{i+1}C_3^*}{a_1b_1}(1-S_5) \quad \text{(B-25)}$$

where

$$S_3=e^{-a_1(\tau-\tau_{Bi})}-e^{-b_1(\tau-\tau_{Bi})} \quad \text{(B-26)}$$

$$S_4=a_1e^{-a_1(\tau-\tau_{Bi})}-b_1e^{-b_1(\tau-\tau_{Bi})} \quad \text{(B-27)}$$

$$S_5=\frac{b_1e^{-a_1(\tau-\tau_{Bi})}-a_1e^{-b_1(\tau-\tau_{Bi})}}{b_1-a_1} \quad \text{(B-28)}$$

$$a_1=2\alpha_{i+1}+\alpha_{i+2}+.5\sqrt{\alpha_{i+2}{}^2+4\alpha_{i+1}^2} \quad \text{(B-29)}$$

$$b_1=2\alpha_{i+1}+\alpha_{i+2}-.5\sqrt{\alpha_{i+2}{}^2+4\alpha_{i+1}^2} \quad \text{(B-30)}$$

The time of breakthrough in the middle layer τ_{Bi+1} is obtained by solving Eq. (B-24) for $X_{i+1} = 1$. The location X_{3LL} of the front in the third layer is obtained by substituting this time in Eq. (B-25). For $\tau > \tau_{Bi+1}$, X_i in Eq. (B-16) is replaced by 1 and it will have the solution becomes

$$X_{i+2}=(X_{3LL}-1-\frac{C_{i+2}^*}{\alpha_{i+2}})e^{-\alpha_{i+2}(\tau-\tau_{Bi+1})}+1-\frac{C_{i+2}^*}{\alpha_{i+2}} \quad \text{(B-31)}$$

The time of breakthrough in the last layer is obtained by setting $X_{i+2} = 1$ in Eq.(B-31) and can be expressed as

$$\tau_{Bi+2}=\tau_{Bi+1}+\frac{1}{\alpha_{i+2}}\ln\left[1+\frac{(1-X_{3LL})}{C_{i+2}^*}\alpha_{i+2}\right] \quad \text{(B-32)}$$

SI Metric Conversion Factors

bbl	x	1.589 873	E – 01 = m^3
cp	x	1.0*	E – 03 = Pa.s
ft	x	3.048*	E – 01 = m
ft^2	x	9.290 304*	E – 02 = m^2

*Conversion factor is exact.